**PHY407 Lab 09**

**Sang Bum Yi, 1004597714**
**Jianbang Lin, 1004970720**

**The workload was distributed as followings:**

- **Sang Bum Yi did question 1**
- **Jianbang Lin did question 2**

## Question 1

**Part a)**

The time-dependent Schrodinger equation, which is defined as equation 1.1 below, was solved using the Crank-Nicolson scheme.

$$i\hbar\frac{\partial\Psi}{\partial t} = \mathcal{H}_D\Psi \qquad \text{[Eq 1.1]}$$

In order to apply the Crank-Nicolson scheme, both space and time were discretized. Consequently, the wavefunction and the Hamiltonian were also discretized as shown in Equation 1.2 and Equation 1.3 respectively.

$$\Psi(t) = \begin{pmatrix} \psi_1(t) \\ \vdots \\ \psi_p(t) \\ \vdots \\ \psi_{p-1}(t) \end{pmatrix} with\ \psi_p(t) = \psi(pa - \tfrac{L}{2}, t) \qquad \text{[Eq 1.2]}$$

$$\mathcal{H}_D = \begin{bmatrix} B_1 & A & 0 & \cdots & 0 \\ A & B_2 & A & \cdots & 0 \\ 0 & \ddots & \ddots & \ddots & \vdots \\ \vdots & 0 & A & B_{p-2} & A \\ 0 & \cdots & 0 & A & B_{p-1} \end{bmatrix} \qquad \text{[Eq 1.3]}$$

where 'L' refers to the total length, 'a' refers to the space distribution, and 'p' refers to the index of the discretization. The elements A and B were computed using equation 1.4 and equation 1.5

$$A = \frac{-\hbar^2}{2ma^2} \qquad \text{[Eq 1.4]}$$

$$B = V\left(pa - \frac{L}{2}\right) - 2A \qquad \text{[Eq 1.5]}$$

The Crank-Nicolson scheme accounts for the time-evolution of the wavefunction by the below expressions which are derived in the instruction.

$$\left(\mathbb{I}_{p-1} + i\frac{\tau}{2\hbar}\mathcal{H}_D\right)\Psi^{n+1} = (\mathbb{I}_{p-1} - i\frac{\tau}{2\hbar}\mathcal{H}_D)\Psi^n \qquad \text{[Eq 1.6]}$$

$$\mathcal{L}\Psi^{n+1} = v \qquad \text{[Eq 1.7]}$$

with $\mathcal{L} = \left(\mathbb{I}_{p-1} + i\frac{\tau}{2\hbar}\mathcal{H}_D\right)$, $v = \mathcal{R}\Psi^n$, $\mathcal{R} = (\mathbb{I}_{p-1} - i\frac{\tau}{2\hbar}\mathcal{H}_D)$ [Eq 1.8]

In part (a), the initial wave function at t=0, which is defined in Equation 1.9, was evaluated over time inside the infinite square well potential in Equation 1.10.

$$\psi(x, t = 0) = \psi_0 \exp\left(-\frac{(x-x_0)^2}{4\sigma^2} + ikx\right) \qquad \text{[Eq 1.9]}$$

where $\sigma = \frac{L}{25}$, $k = \frac{500}{L}$, $and\ x_0 = L/5$

$$\text{V(x)} = \begin{cases} = 0, & -\frac{L}{2} < x < \frac{L}{2} \\ = \infty, & x \leq -\frac{L}{2}\ or\ \frac{L}{2} \leq x \end{cases} \qquad \text{[Eq 1.10]}$$

In order to ensure that the energy is constant and the wave function remains normalized over time, the energy and the normalization were computed using equation 1.11 and 1.12, respectively. Using the computed values, energy and normalization graphs were produced as shown in Figure 1.1 and Figure 1.2, respectively. Note that both are kept at the same value over time, which mean the energy is constant and the normalization is equal to 1 as expected.

$$E(t) = \int_{-\infty}^{\infty} \psi^*(x,t)\mathcal{H}_D\psi(x,t)dx \qquad \text{[Eq 1.11]}$$

$$\int_{-\infty}^{\infty} \psi^*\psi dx = 1 \qquad \text{[Eq 1.12]}$$

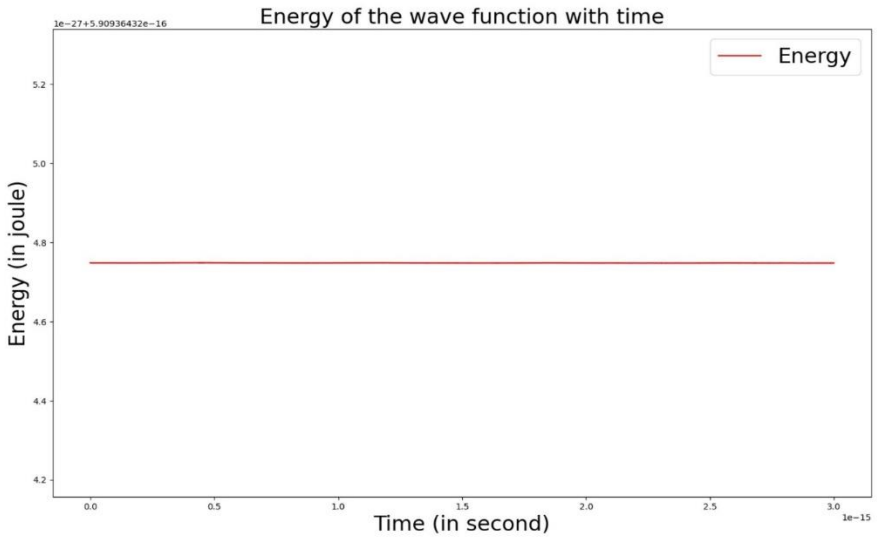


*Figure 1.1: Energy versus time. The horizontal line implies the energy being constant over time. Each time step is $\tau = 10^{-18}s$ and a total of 3000 time points are plotted.*

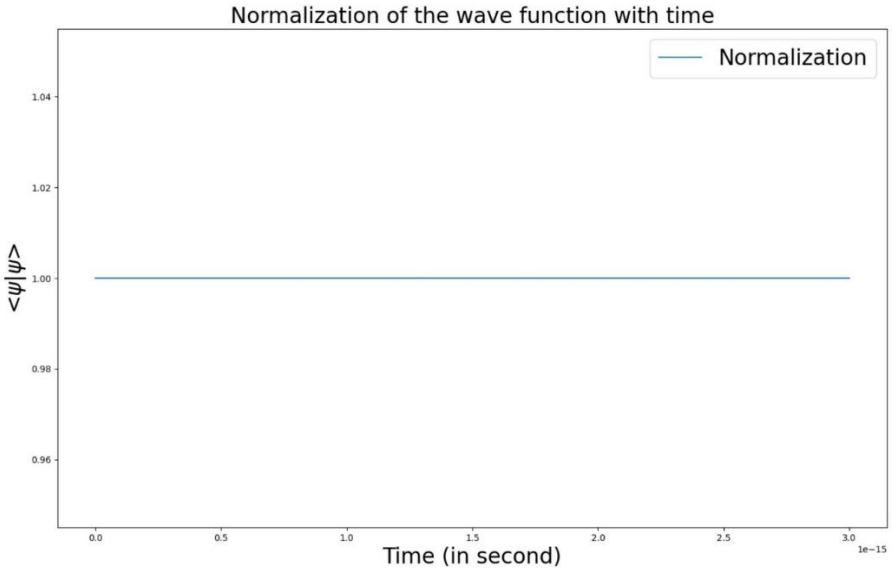


*Figure 1.2: Normalization versus time. Note that the normalization is kept at 1, as it should be. Each time step is $\tau = 10^{-18}s$ and a total of 3000 time points are plotted.*

The computation of both energy and normalization was done by matrix manipulation. Given the discretized Hamiltonian $\mathcal{H}_D$ is 1024 x 1024 matrix and $|\psi(x,t)>$ is 1024 x 1 matrix, the expected energy is expressed in bra-ket notation as $< E(t) > = < \psi(x,t)|\mathcal{H}_D|\psi(x,t) >$. Similarly, the normalization was computed by multiplying the bra $< \psi(x,t)|$, which is 1 x 1024 matrix, with the ket $|\psi(x,t)>$, which is 1024 x 1 matrix. The matrix manipulation was done by using built-in functions in numpy such as numpy.matmul(A, B) for matrix multiplication and numpy.conj(A) for matrix conjugation.

**Part b)**

Given the wave functions inside the infinite square well potential from part (a), the probability density $\psi^*\psi$ was computed by taking square of its absolute value at each time step. In addition, its trajectory <X>(t), which is expressed in Equation 1.13, was computed by diving the sum of the product of the position and the probability density by the total number of space points. Figure 1.3 shows the trajectory of the average position over time.

$$< X > (t) = \int_{-\infty}^{\infty} \psi^*(x,t) x \psi(x,t) dx \qquad \text{[Eq 1.13]}$$

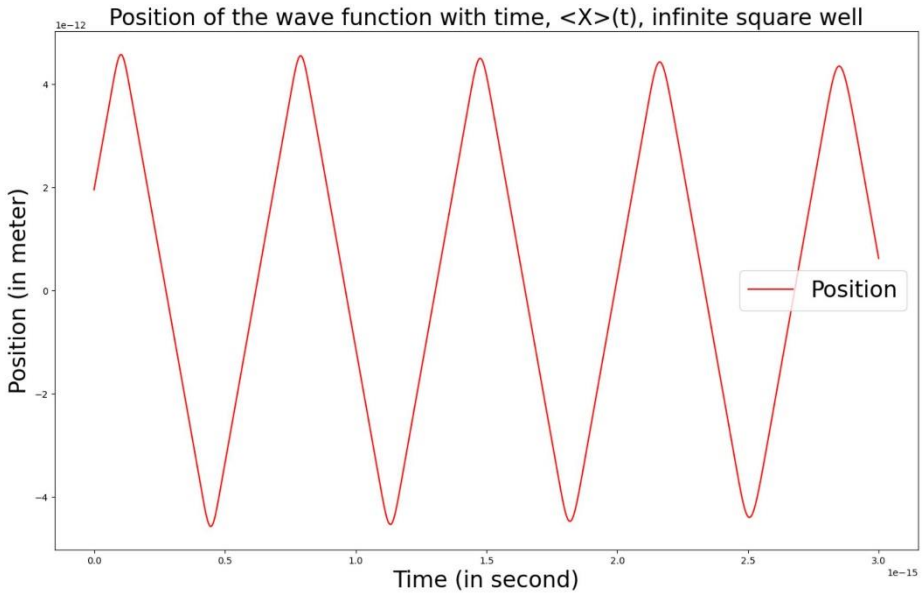


*Figure 1.3: Average position over time in an infinite square well potential. Note that the trajectory oscillated back and forth inside the boundaries [-L/2, L/2]*

The oscillation in figure 1.3 can be explained using one of the consequences of the Ehrenfest Theorem, which states that "if the wave function is highly concentrated around a point $x_0$, then V'(<x>) and <V'(x)> will be almost the same. In that case, the expected position will approximately follow the classical trajectories". Since the infinite square potential gives V(x) = 0 everywhere inside the boundaries, the wavefunction is highly concentrated at a certain point and V'(<x>) and <V'(x)> are the same. Therefore, agreeing with the theorem, the trajectory of the average position follows the classical trajectory as shown in Figure 1.3

The plot of the probability density $\psi^*\psi$ over time was animated and can be found in "Infinite_Square_Well.mp4". In the animation, the probability density shows a gaussian-like distribution that has the highest peak at a certain position and travels back and forth inside the boundaries x = -L/2 and x = L/2. When it hits the boundaries, the probability density crushes like the wave on the beach but eventually bounces back and travels into the opposite direction toward the other boundary. Furthermore, the magnitude of the highest peak keeps decreasing as it hits the

boundaries and the width of the distribution becomes larger, which means the localization of the wave function becomes weaker.

**Part c)**

In part (c), the infinite square well potential was replaced by the harmonic oscillator in Equation 1.14 below. Therefore, the discretized Hamiltonian matrix $\mathcal{H}_D$ was generated using the new value of B in Equation 1.5 and the frequency $\omega = 3 * 10^{15} s^{-1}$. The wave function was calculated using the same $x_0$, but integrated over 4000 time steps.

$$V(x) = \begin{cases} = \frac{1}{2} m\omega^2 x^2, & -\frac{L}{2} < x < \frac{L}{2} \\ = \infty, & x \leq -\frac{L}{2} \; or \; \frac{L}{2} \leq x \end{cases} \qquad \text{[Eq 1.14]}$$

Then the probability density $\psi^* \psi$ and its trajectory <X>(t) were computed using the same method in part (b). The trajectory <X>(t) was plotted as shown in Figure 1.4

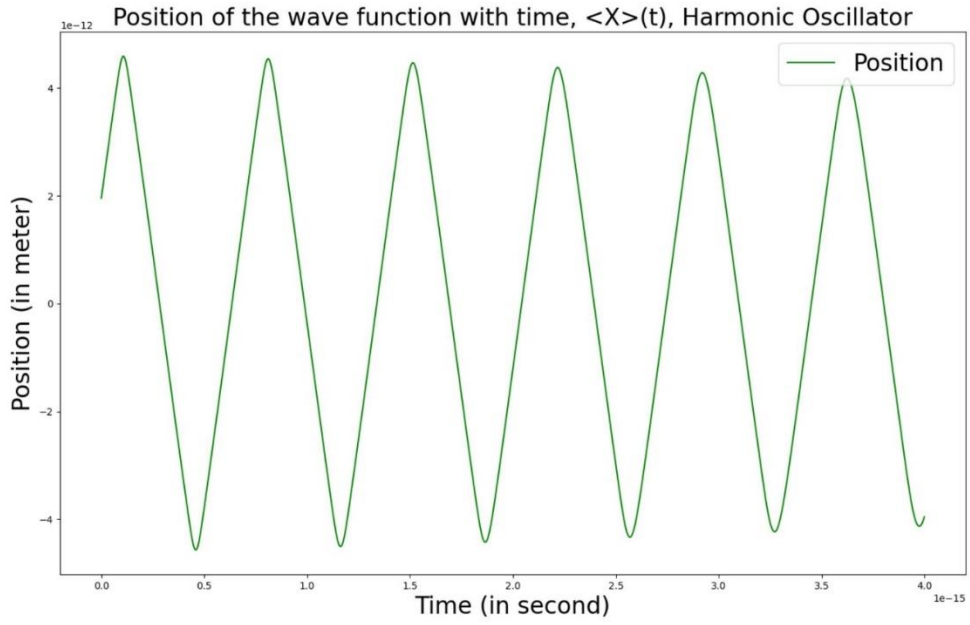


*Figure 1.4: Average position over time in an harmonic oscillator potential. Note that the trajectory oscillated back and forth inside the boundaries [-L/2, L/2]*

Again, the trajectory in Figure 1.4 oscillates between the boundaries much like a classical trajectory, which agrees with the Ehrenfest theorem.

Similarly, the plot of the probability density $\psi^* \psi$ over time was animated and can be found in "Harmonic_Oscillator.mp4". The behaviour of the wave function is much like that of the wave

function in the infinite square well potential. At first, it starts with a localization at $x_0$ and oscillates back and forth inside the boundaries, decreasing the magnitude of its highest peak and increasing the width of the distribution. It also shows the similar crushing pattern when it hits the boundaries because the wave function goes to zero at the infinite potential.

**Part d)**

In part (d), the infinite square well potential was replaced by double well potential in Equation 1.15 below. Therefore, the discretized Hamiltonian matrix $\mathcal{H}_D$ was generated using the new value of B in Equation 1.5. The wave function was integrated over 6000 time steps.

$$V(x) = \begin{cases} = V_0(\frac{x^2}{x_1^2} - 1)^2, & -\frac{L}{2} < x < \frac{L}{2} \\ = \infty, & x \leq -\frac{L}{2} \; or \frac{L}{2} \leq x \end{cases} \qquad \text{[Eq 1.15]}$$

where $V_0 = 6 * 10^{-17} J$, $x_0$ = L/3, and $x_1$ = L/4

Then the probability density $\psi^* \psi$ and its trajectory <X>(t) were computed using the same method in part (b). The trajectory <X>(t) was plotted as shown in Figure 1.5.

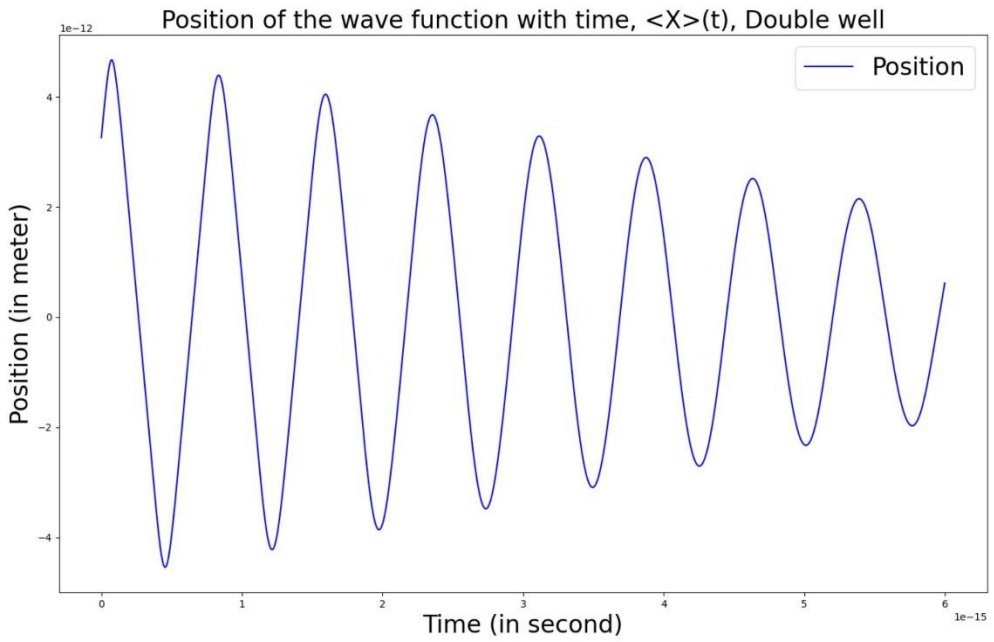


*Figure 1.5: Average position over time in a double well potential. Note that the magnitude of the average position decreases over time.*

Unlike the trajectories of the infinite square well and harmonic oscillator potential, the trajectory of the average position inside the double well potential decreases its magnitude over time. This phenomenon can also be observed in the animation of the probability density $\psi^* \psi$, which is

"Double_Well.mp4". The crush of the wave function at the boundaries is much more intense in the case of the double well potential, therefore making the wavefunction less localized much faster than the other two cases. Toward the end of the animation, the wave function becomes almost flat and purely wave form with no localization at all. This is again expected by Ehrenfest Theorem because the potential V'(<x>) and <V'(x)> are not equal anymore, which makes the trajectory not follow the classical trajectory.

## Question 2

The electric and magnetic fields within a 2D cavity with conducting walls can be written as:

$$\vec{E}=\begin{pmatrix}0\\0\\E_z(x,y,t)\end{pmatrix} \quad and \quad \vec{B}=\begin{pmatrix}B_x(x,y,t)\\B_y(x,y,t)\\0\end{pmatrix} \qquad \text{[eq 2.1]}$$

Maxwell's equations state that:

$$\frac{\partial H_x}{\partial t}+c\frac{\partial E_z}{\partial y}=0 \qquad \text{[eq 2.2a]}$$

$$\frac{\partial H_y}{\partial t}+c\frac{\partial E_z}{\partial x}=0 \qquad \text{[eq 2.2b]}$$

$$\frac{\partial E_z}{\partial t}+c\frac{\partial H_y}{\partial x}+c\frac{\partial H_x}{\partial y}=J_z \qquad \text{[eq 2.2c]}$$

Where c is the speed of light, $H_x = cB_x$, $H_y = -cB_y$, $J_z = -\mu_0 c^2 j_z$. By using discrete sine transforms and discrete cosine transforms, the following equations can be obtained.:

$$(E_z)^n_{p,q}=\sum_{q'=0}^{P}\sum_{p'=0}^{P}\widehat{E}^n_{p',q'}\sin\left(\frac{pp'\pi}{P}\right)\sin\left(\frac{qq'\pi}{P}\right) \qquad \text{[eq 2.3a]}$$

$$(H_x)^n_{p,q}=\sum_{q'=0}^{P}\sum_{p'=0}^{P}\widehat{X}^n_{p',q'}\sin\left(\frac{pp'\pi}{P}\right)\cos\left(\frac{qq'\pi}{P}\right) \qquad \text{[eq 2.3b]}$$

$$\left(H_y\right)_{p,q}^{n} = \sum_{q'=0}^{P}\sum_{p'=0}^{P} \widehat{Y}_{p',q'}^{n} \cos\left(\frac{pp'\pi}{P}\right)\sin\left(\frac{qq'\pi}{P}\right) \qquad \text{[eq 2.3c]}$$

**Part a)**

The boundary conditions in this question are given:

1. $E_z$ = 0 at x=0, $L_x$ and y=0, $L_y$
2. $H_x = \partial_x H_y = 0$ at x=0, $L_x$
3. $H_y = \partial_y H_x = 0$ at y=0, $L_y$

To verify boundary condition 1, for equation 2.3a, when x=0, p=0, this will make $\sin\left(\frac{pp'\pi}{P}\right)$ = 0, thus making $E_z$ = 0. When x=$L_x$, p=P, $\sin\left(\frac{pp'\pi}{P}\right) = \sin(p'\pi) = 0$, therefore $E_z$ = 0.

To verify boundary condition 2, for equation 2.3b,
$\partial_x H_y = \sum_{q'=0}^{P}\sum_{p'=0}^{P} \widehat{Y}_{p',q'}^{n} - \frac{p'\pi}{P}\sin\left(\frac{pp'\pi}{P}\right)\sin\left(\frac{qq'\pi}{P}\right)$, since $\sin\left(\frac{pp'\pi}{P}\right)$ = 0 when x=0, $L_x$, therefore $H_x = \partial_x H_y = 0$

To verify boundary condition 3, for equation 2.3c,
$\partial_y H_x = \sum_{q'=0}^{P}\sum_{p'=0}^{P} \widehat{X}_{p',q'}^{n} - \frac{q'\pi}{P}\sin\left(\frac{pp'\pi}{P}\right)\sin\left(\frac{qq'\pi}{P}\right)$, since $\sin\left(\frac{qq'\pi}{P}\right)$ = 0 when y=0, $L_y$, therefore $H_y = \partial_y H_x = 0$.

**Part c)**

The driving current inside cavity is given by:

$$J_z(x,y,t) = J_0 \sin\left(\frac{m\pi x}{L_x}\right)\sin\left(\frac{n\pi y}{L_y}\right)\sin(\omega t) \qquad \text{[eq 2.4]}$$

When driving current has frequency ω=3.75, the graph for $E$, $H_x$, $H_y$ at point $E(x = 0.5, y = 0.5)$, $H_x(x = 0.5, y = 0)$, $E(x = 0.5, y = 0.5)$ is following:

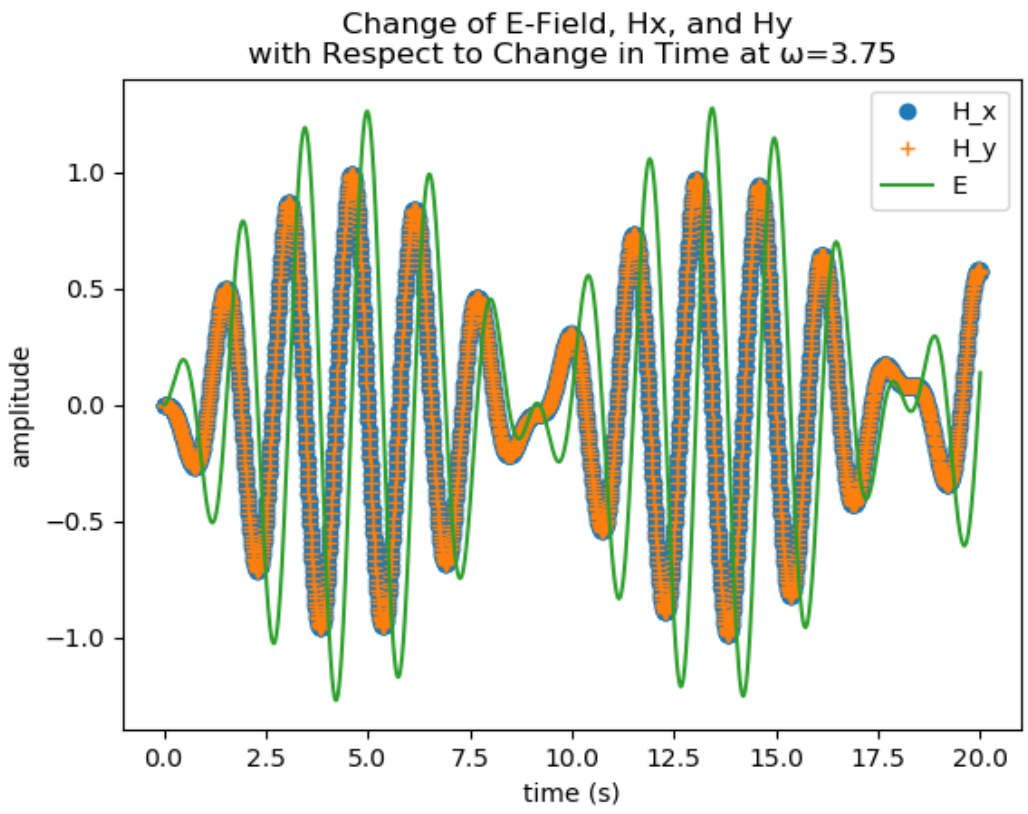


*Figure 2.1: Change of $E$, $H_x$, $H_y$ at point $E(x = 0.5, y = 0.5)$, $H_x(x = 0.5, y = 0)$, $E(x = 0.5, y = 0.5)$ with driving current of frequency 3.75 between time 0s and 20s.*

This graph shows that the $E$, $H_x$, and $H_y$ are periodic, and $H_x$, $H_y$ are overlapped with each other. By tracing their maximum amplitude, they form an oscillating pattern as well. Also, $E$ and $H$ have the same frequency. The oscillation of maximum values is caused by driving current J. When $E$ points in the same direction of J, $E$ and $H$ will grow stronger, however, if they are different in direction, $E$ and $H$ will grow weaker. Since $E$ and J do not have the same frequency, that is why the maximum amplitude of $E$ and $H$ will vary and have an oscillating shape.

**Part d)**

The maximum value of E varies with frequency, and the following graph shows the maximum amplitude of electric field with different frequency:

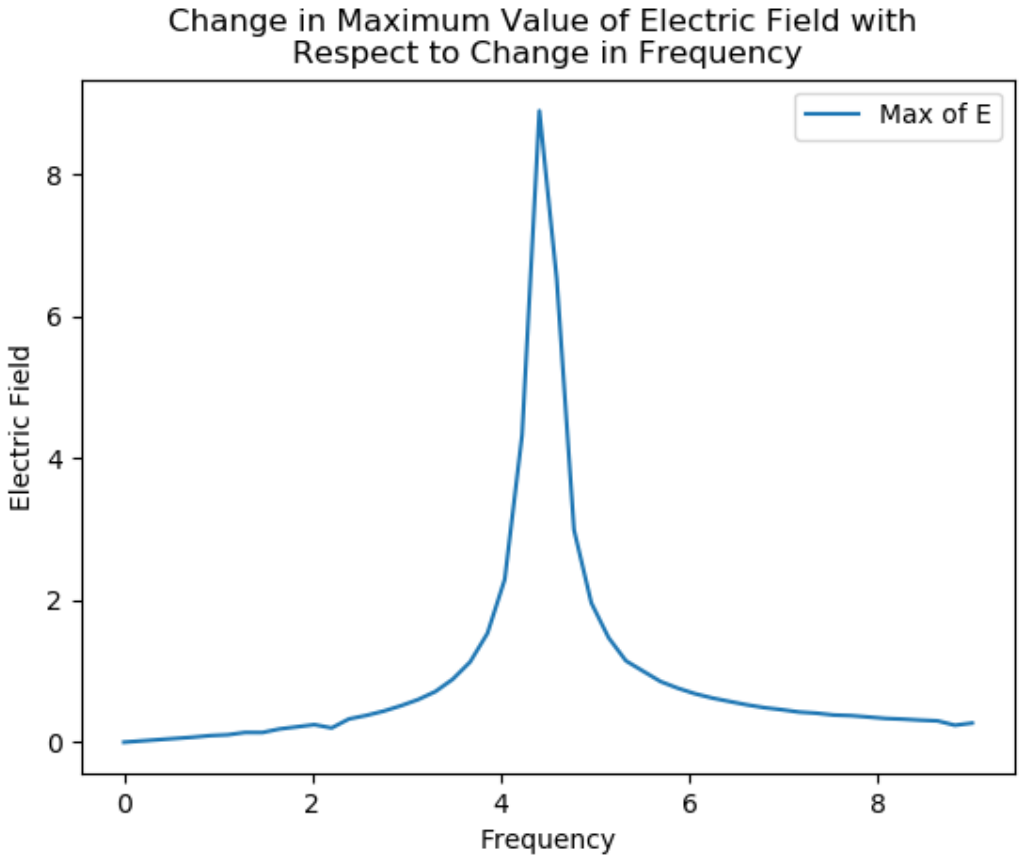


*Figure 2.2: Change in maximum amplitude in electric field with respect to change in driving current frequency.*

This graph shows that the maximum amplitude of electric field occurs when frequency is around 4.5.

The normal frequencies of this system is given by:

$$\omega_0^{m,n} = \pi c \sqrt{\left(nL_x\right)^{-2} + \left(mL_y\right)^{-2}} \qquad \text{[eq 2.5]}$$

Therefore, at the amplitude peaks when n and m are 1 and 1.

**Part e)**

When $\omega = \omega_0^{m,n} = \sqrt{2}\pi$, the graph for $E$, $H_x$, $H_y$ at point $E(x = 0.5, y = 0.5)$, $H_x(x = 0.5, y = 0)$, $E(x = 0.5, y = 0.5)$ is following:

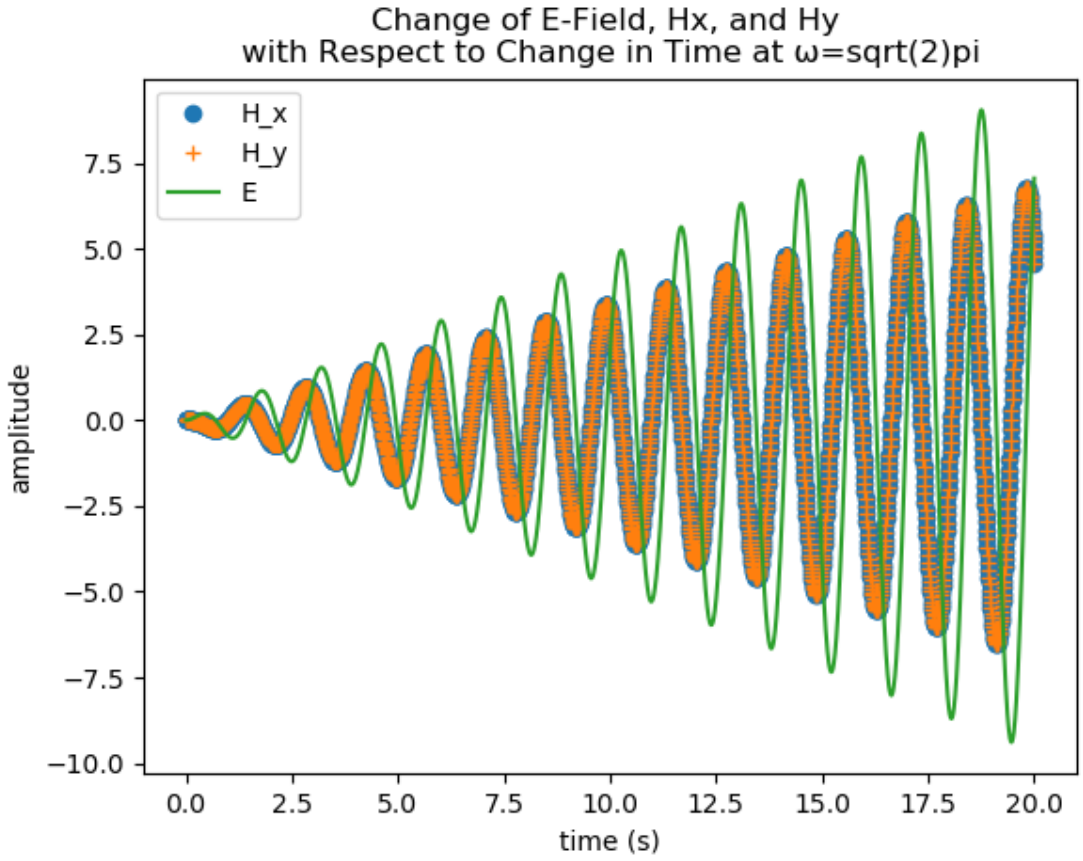


*Figure 2.3 Change of $E$, $H_x$, $H_y$ at point $E(x = 0.5, y = 0.5)$, $H_x(x = 0.5, y = 0)$, $E(x = 0.5, y = 0.5)$ with driving current of frequency sqrt(2)pi between time 0s and 20s.*

This graph shows that amplitude of electric field, $H_x$, and $H_y$ increase with time, this is because the frequencies of $E$, $H_x$, $H_y$ are very close to frequency of driving current J, this is similar to the phenomenon of resonance. Compared with graph 2.1, the main difference is that in graph 2.1, the maximum values of oscillation are periodic, but the maximum values of oscillation in 2.3 are not, they increase with time.

Since the energy of a system is proportional to the magnitude of the electric field, therefore, the energy in the cavity increases with time.